PROCEEDINGS OF THE BELGIAN ROYAL ACADEMIES OF MEDICINE

www.probram.be

Three-dimensional rapid prototyping models in cranio-maxillofacial surgery: systematic review and new clinical applications

Raphael Olszewski

Oral and maxillofacial surgery research Lab (Omfs Lab), Department of Oral and maxillofacial surgery, Cliniques universitaires saint Luc, Université catholique de Louvain, Av. Hippocrate 10, 1200 Brussels, Belgium.
Tel: + 32-2-7645718
Fax: + 32-2-7645876
Email: raphael.olszewski@uclouvain.be

Received: 04.07.2012 Accepted: 18.09.2012 Published: 28.03.2013

Abstract

Medical models represent portions of human anatomy obtained from three-dimensional (3D) medical imaging. The aim was to provide a current review of clinical applications, technical accuracy and artefacts explanation with rapid prototyping (RP) technologies in cranio-maxillofacial (CMF) surgery. We also presented new RP clinical applications in reconstructive, orthognathic, and malformative CMF surgery. A systematic review of the literature was conducted on PubMed, and based on title-abstract sifting by one observer. Inclusion criteria consisted of medical rapid prototyping, 3D models, stereolithography, selective laser sintering, fused deposition modelling, 3D printing, polyjet, maxillofacial, craniofacial, cranioplasty, and implantology. In total we found 573 articles and 96 were retained for this review. Four principal sources of 3D models for clinical applications in CMF surgery are stereolithography, selective laser sintering, 3D printing, and fused deposition modeling. 3D models were used in most of domains of CMF surgery such as: reconstructive, orthognathic, temporo-mandibular surgery, craniofacial malformations, cranioplasty, and implantology. Majority of selected articles presented with a low level of evidence (level 4, case series and case reports). Problems with costs of models and machines, toxicity of material used to build up the model, need of multidisciplinary expertise still limit the use of 3D RP models to complex cases and to university hospitals teams. Further research should be directed toward ecological low-cost 3D RP techniques providing an accuracy acceptable with its clinical use. Randomized control trials should be developed to prove the usefulness of 3D RP models in CMF surgery.

Keywords: *maxillofacial surgery, rapid prototyping, three-dimensional, anatomic models, review*

INTRODUCTION

Medical models or bio-models represent portions of human anatomy at a scale of 1:1 obtained from three-dimensional (3D) medical imaging (CT scan, MRI). The procedure for the fabrication of medical models consists of multiple steps: 1) the acquisition of high-quality volumetric 3D image data of the anatomical structure to be modelled, 2) 3D image processing to extract the region of interest from surrounding tissues, 3) mathematical surface modelling of the anatomic surfaces, 4) formatting of data for rapid prototyping (RP) (this includes the creation of model support structures that support the model during building, which are subsequently manually removed), 5) model building, and 6) quality assurance of the model and its dimensional accuracy. These steps require significant expertise and knowledge of medical imaging, 3D medical image processing, computer-assisted design, and software manufacturing and engineering processes. The production of reliable, high-quality models requires a team of specialists that may include medical imaging specialists, engineers, and surgeons (1). Rapid prototyping was introduced in the 1980's to define new techniques for the manufacturing of physical models based on CAD-CAM (computer-aided design, computer-aided manufacturing). RP technology allows the building of a medical model layer by layer, reproducing almost every form of the external and internal anatomic structure. Other categories of RP technologies are solid freeform fabrication, layer additive manufacturing, and 3D printing. RP techniques are different from physical models obtained by milling. RP medical modelling in cranio-maxillofacial (CMF) surgery has mainly been developed over the last ten years (Phidias European network), and concerns the following range of applications: 1) aiding in the production of surgical implants, 2) improving surgical planning, 3) acting as an orientation aid during surgery, 4) enhancing diagnostic quality, 5) using in preoperative simulation, 6) achieving a patient's consent prior to surgery, and 7) preparing a template for resection for surgeons (2). Almost all of the RP techniques that have been developed were used in CMF surgery, and these will be presented in the following literature review. These techniques include stereolithography (SL), selective laser sintering (SLS), fused deposition modelling (FDM), 3D printing (3DP), and polyjet modelling.

MATERIALS AND METHOD

A systematic review of the literature was conducted on PubMed (Medline). A search strategy employed was based on title-abstract sifting by one observer. Our exclusion criteria consisted of general dentistry, prosthodontics, orthodontics, forensic medicine, orthopaedics, biomechanics, tissue engineering, finite element analysis, virtual imaging, and animal studies. The inclusion criteria consisted of medical rapid prototyping, three-dimensional models,

stereolithography, selective laser sintering, fused deposition modelling, 3D printing, polyjet, maxillofacial, craniofacial, cranioplasty, and 3D models-based implantology guides. The search strategy was based on eight search formulas that combined free terms and MeSh terms:
1) ((RP[All Fields] AND models[All Fields]) AND maxillofacial[All Fields] AND ("humans"[MeSH Terms] AND English[lang])) (search on 15.03.11), with 10 articles found, 2 articles excluded, and 8 articles selected;
2) ((Medical[All Fields] AND rapid[All Fields] AND prototyping[All Fields]) AND (maxillofacial[All Fields] OR craniofacial[All Fields]) AND ("humans"[MeSH Terms] AND English[lang])) (search on 17.03.11), with 24 articles found, 9 articles excluded, and 15 articles selected;
3) ((three-dimensional[All Fields] AND models[All Fields]) AND (maxillofacial[All Fields] OR craniofacial[All Fields]) AND ("humans"[MeSH Terms] AND English[lang] AND (hasabstract[text])) (search on 17.03.11 to 19.03.11), with 480 articles found, 402 articles excluded, and 78 articles selected;
4) ((stereolithography[All Fields] AND maxillofacial[All Fields] AND ("humans"[MeSH Terms] AND English[lang])) (search on 15.03.11), with 38 articles found, 12 articles excluded, and 26 articles selected;
5) ((Selective laser sintering [All Fields] AND maxillofacial[All Fields] AND ("humans"[MeSH Terms] AND English[lang])) (search on17.03.11), with 9 articles found, 2 article excluded, and 7 articles selected;
6) (fused deposition modelling [All Fields] AND maxillofacial[All Fields] AND ("humans"[MeSH Terms] AND English[lang])) (search on 17.03.11), with 1 article found, and 1 article selected;
7) ((three[All Fields] AND dimensional[All Fields]) AND (printer[All Fields] OR ("printing"[MeSH Terms] OR "printing"[All Fields])) AND maxillofacial[All Fields] AND ("humans"[MeSH Terms] AND English[lang]) (search on 15.03.11), with 10 articles found, 4 articles excluded, and 6 articles selected; and
8) (polyjet[All Fields] AND (maxillofacial[All Fields] OR craniofacial[All Fields]) AND ("humans"[MeSH Terms] AND English[lang]) (search on 17.03.11), with 1 article found, and 1 article selected.

The limits were human studies, English language, and articles with abstract. There were no limits for the time of publication. After title-abstract sifting the total number of articles found was 573, with 431 articles excluded, and 141 articles selected. The number of duplicate article found among the eight search formulas was 45. Finally, we selected 96 articles for review.

RESULTS

Among the selected articles 78 articles (2-80) corresponded to stereolithography, 9 articles (81-90) to selective laser sintering, 1 article (91) to fusion deposition modelling, 9 articles (48, 54, 89, 90, 92-96) to 3D printing, and 1 article (90) to polyjet modeling. The level of evidence for all selected articles was poor with a level 4 (on a scale from 1 to 5) for 90 articles (37 case series, 42 case reports, 10 non systematic reviews, 1 case-controlled study of poor quality). There were also 6 articles not concerned by the quality appraisal (in vitro technique assessment).

DISCUSSION

STEREOLITHGRAPHY (SL)

Stereolithography: clinical applications

Stereolithography has been the most used RP technique in CMF surgery since it was first applied in grafting a skull defect in 1994 (3-6). SL models have been used as preoperative planning tools for maxillofacial fractures reduction and ostesynthesis, in craniofacial syndromes and correction of asymmetric faces, in orthognathic surgery, in distraction osteogenesis, in post-tumoral reconstructive surgery, in temporo-mandibular joint (TMJ) surgery, in skull defects reconstruction and cranioplasty, and in implantology (7). This technique can also be used for ear or orbital reconstruction and could be potentially applied in anthropological studies or in the study of facial aging (7). Selectively colored SL models have been used for the diagnosis and planning of treatments related to supernumerary teeth extraction in cleidocranial dysplasia (8), in planning of complex maxillofacial or intracranial tumor surgery (9, 10), and for the visualisation of rapports between the disc and mandibular condyle in the TMJ (11).

SL models may assist in the diagnosis of and preoperative planning for facial fractures (12), especially in late primary repair, when open reduction and internal fixation have to wait for a decrease in facial swelling or cerebral edema. SL models facilitate anatomical reduction, minimise surgical approaches, save operating time, and lead to improvement of postoperative results, which may reduce the number of secondary corrections required for late post-traumatic deformities (13-15). In secondary reconstruction of zygomatic complex SL model allows for analysis of the actual displacement of bone in 3D and can be employed to plan a surgery and move the zygoma to its final ideal position. Using these models, osteosynthesis plates can be individually prebent before actual surgery, thereby shortening operating time. To transfer the preoperative plan to the operating theatre, a 3D CT-based navigation system can be associated with SL models to transfer the exact positions of the screws from the SL model to the patient (15). However, SL models have proven to be less useful in cases of consolidated fractures of the periorbital and naso-ethmoidal complex, except where there is major dislocation, because of the limited representation of detailed structures (sutures) present in this region (16).

SL models can serve for preoperative planning in malformative craniofacial syndromes (17), in which the visualization of complex anatomy may considerably modify the surgical approach applied, as well as avoiding unnecessary complications (18-23). SL models were also used to follow-up of craniofacial growth in craniofacial syndromes (24). SL models have provided additional relevant anatomical information related to hypertelorism, severe asymmetries of the neuro- and viscerocranium, complex cranial synostoses and large skull defects (25). In hemifacial microsomia Zhou et al. (26) developed a customised mandibular implant model that was designed in a computer-assisted manner by projecting a mirror image of the healthy mandible onto the affected side in a 3D CT model. SL model of the mirrored mandible was then prepared. Finally, a polymeric biomaterial was sculpted according to that SL model and implanted into the affected side of the mandible to restore the patient’s facial symmetry (25, 26). The value of these models as realistic "duplicates" of complex or rare dysmorphic craniofacial pathologies for the purpose of creating a didactic collection should also be emphasised (16). However, SL models representing only bone do not reveal the spatial relationships between soft tissue and bone in complicated craniofacial deformities. Therefore, a mixed SL model has been developed showing both soft and bony tissue by first using CT values, resulting in a model in which soft tissue is solid and bone is replaced by empty space (27). The space is then filled with plaster to represent the skeleton. This model also can provide baseline data for evaluating facial growth after surgical repair of clefts (27, 28).

The goal of orthognathic surgery is to treat sagittal, vertical or transverse skeletal congenital or post-traumatic dysmorphoses. Orthognathic surgery is based on different types of osteotomies of the maxilla/and or mandible, and allow for modifying the relative position of the maxilla to the mandible, and the absolute position of both the maxilla and mandible to the skull base. Orthognathic surgery is almost associated with pre- and post-surgery orthodontic treatment, as the stable occlusion between the jaws is one of the main goals of the treatment. In orthognathic surgery, SL models replicate the facial skeleton with precise internal anatomy, which can facilitate the design of the osteotomy, the transfer of osteotomy lines to the operating theatre by means of SL-based guides (29, 30) and the preparation for osteosynthesis. Each sectioned segment of the maxilla and mandible can be accurately repositioned by transferring the positional relationships of multiple reference points on the SL model to the bone surface using pre-bent titanium plates (31). Efforts have been made to replace CT-images, which are often affected by artefacts (due to metallic dental amalgams), thus resulting in poor representation of the tooth area in SL models, as occlusion plays a major role in orthognathic surgery in terms of aesthetics, and in avoiding postoperative relapse. Therefore, hybrid SL models based on scanning of plaster casts and on skull CTs have been obtained to allow for more accurate planning of orthognathic surgeries (32). Finally, SL technique allows the generation of digital templates that are used during surgery to assist the surgeon in repositioning the maxilla and/or the mandible in relation to each other (33).

Distraction osteogenesis is a surgical process used to reconstruct skeletal deformities and lengthen long bones of the body. A corticotomy is used to fracture the bone into two segments, and the two ends of the bone are gradually drawn (with a distraction device) apart during the distraction phase, allowing new bone to form in the gap. When the desired or possible length is reached, a consolidation phase follows, in which the bone is allowed to continue healing (34). Distraction osteogenesis has the benefit of simultaneously increasing bone length and the volume of surrounding soft tissues. Its application to the craniofacial skeleton allowed for better corrections of multiple complex maxillomandibulary craniofacial deformities to be achieved. SL models have been used preoperatively to: 1) evaluate various surgical options (34, 35), 2) simulate osteotomies and the positioning of the distractor device (36), 3) prebend plates or inserts of the distraction device (37, 38), 4) define the vector of distraction (the direction of the movement of the elongated bone), 5) simulate final results (39, 40) and, 6) develop a surgical guide to transfer a surgical plan (osteotomy lines, and the positions of inserts on both sides of the distracted area) to the operating theatre (36). If the distractor is to be prepared for mandibular elongation, the position of the screws (inserts) can be determined preoperatively according to growth trends, to the location of the tooth buds and, to inferior alveolar nerve (41). In correcting mandibular micrognathia and TMJ ankylosis in particular (41), 3D SL models have several advantages: 1) the range of bilateral TMJ ankylosis and the position of the osteotomy line can be easily determined; 2) the transport disc can be designed at the posterior edge of the mandibular ramus, with individual, tailored ramus distractors being made; 3) the precise distraction length of the bilateral mandible body can be determined for later orthodontic therapy and orthognathic surgery; 4) the position of the osteotomy line in the mandible body can be determined, with an individual tailored distractor being made; 5) for immobilization, the attachment plate of the distractor can be adjusted and attached to the surface of the mandible; and 6) surgical procedures can be explained clearly to patients using the 3D model.

Moreover, SL models can be used for preoperative planning of maxillary resection due to oral cancer (42) and for the planning of maxillary reconstruction with osseo-cutaneous microvascularised free-flaps. A SL model can serve to: 1) visualise the extent of a tumor (43), 2) evaluate the anatomy of a defect, and define the residual anchor bone for integration with free-flap segments (44), 3) design osteotomies based on free-flaps and the direction of segment replacement to simulate symmetric maxilla reconstruction (44), 4) fit a graft exactly, with or without reduced reshaping (44), 5) pre-adapt plates based on a SL model (45), 6) manufacture a surgical guide for tumoral resection (46), 7) shorten the surgical time before a free-flap is re-anastomosed and reduce the risk of microsurgery (44), 8) predict the outcome of surgery (44), 9) provide a permanent record for future needs or reconstructions (43). SL models have also been used for the preoperative planning of mandibular resection and reconstruction (47). Mandibular reconstruction is often needed after partial resection and due to continuity defects (48). The aims for the reconstruction are maintaining the proper aesthetics and symmetry of the face and achieving of a good functional result, thus preserving the shape and the strength of the jaw and allowing future dental rehabilitation (48). Reconstruction poses multiple challenges for the maxillofacial surgeon, such as the complicated geometry of the mandible, the muscles attached to the mandible, which act in different directions, the shape and position of the condyles in the glenoid fossa, and occlusion (48). Reconstruction of the mandible can be achieved using a temporary bridging titanium locking bone plate until bony reconstruction of the gap is accomplished (48). The use of the reconstruction plate is also advocated when predicted life expectancy is low and when medical conditions preclude prolonged general anaesthesia (48). Further rehabilitation of the mandible can be performed using autogenous bone grafting (iliac crest, fibula free-flap), which is a reliable standard procedure (48). Incorporation of the bone graft into the mandible provides the continuity and strength necessary for its proper functioning, with the possibility of dental implant rehabilitation (48). Bone tissue can be harvested during the first surgical procedure or at a later stage (48). SL 3D models of the mandible are used to assist in developing a presurgical plan, including consideration of the length of the resection (49). On the SL model, the mandibular and mental foramina are marked, the course of the mental nerve is demarcated, and the boundaries of the mandibular resection are chosen. The reconstruction plate is premolded to the planned neo-mandible model (50). Intra-operative time is expended moulding the plate imprecisely. Instead, the plate can be bent on SL model as exactly as possible before the surgery without the pressure of time. This method serves as a valuable learning tool for junior surgeons. Patients can also gain a significantly better understanding of the problem and the challenges of reconstruction by using such models, which results in a better alignment of hopes and expectations between patients and surgeons. Some potential drawbacks of these techniques include the cost of SL models and the difficulty in adapting them to situations in which the surgical plan changes intra-operatively (i.e., tumour-positive bone margins demanding a larger bone resection). Plates (49), trays (47), or titanium mesh cages for iliac bone (51), can be easily bent and adapted to fit a mandibular SL models (26, 49). SL model also enable the surgeon to determine the required length of a plate, and the length and number of screws (49). As a result, before resection, there is an accurately fitted and contoured reconstruction plate ready for placement. Decreased exposure time to general anaesthesia, decreased blood loss, and lessened wound exposure time are all significant patient benefits from reduced operating times (49). The ability to complete nonsurgical aspects of a patient’s treatment in the laboratory also allows for precision that is often not achievable during the operative procedure (49).

Reconstruction of major surgical defects in the oral cavity after oncological resections requires the use of a free flap. Vascularised free fibular flaps are considered the most suitable choice for mandible reconstruction because of their favorable aesthetics and their functional outcomes. Fibular bone allows the planning of osteotomies in relation to the orientation of the bone and to its vascular pedicle. Thick cortical bone readily accepts plates and screws for secure inter-osseous fixation, and osteointegrated implants may be placed in this bone safely (52). The length of bone that can be removed is up to 25 cm; the bone may be osteotomised in two to four fragments, and retains its vitality. Other tissue structures such as the skin, fascia, and muscle, can be removed with the bone. A fibula free-flap graft has to be contoured to fit the mandibular defect, so preoperative planning is required. Shaping of the fibular graft can be performed using computer-aided design and computer-aided modeling procedures for evaluation of the presurgical anatomy, whereby 3D SL models of the fibula graft are obtained (52). Three-dimensional SL models of the fibula graft allow for selecting the best titanium plates for each case and bending the plates preoperatively, which reduces the time spent in the operating theatre.

Finally, SL models have also been used for preoperative planning and to guide the bending of titanium plates to be used in the resection of mandibular osteosarcoma (53), osteochondroma of the mandibular condyle (54), coronoid hyperplasia (55), and benign tumors with mandibular bone involvement such as ameloblastoma (56).

The TMJ surgery is mainly performed to treat mandibular condyle fractures, degenerative osteoarthritic diseases, congenital aplasia, temporo-mandibular ankylosis, and TMJ tumors. SL models based on CT imaging (57) or MRI (11) can help in the visualisation of bony structures and the shape of the articular disc in relation to bony structures (11). SL models can also serve in constructing a custom-made, total TMJ prosthesis that is adapted surgically to a patient's unique anatomy (58, 59).

Additionally, SL models have been used for patients with skull bony defects requiring corrective cranioplasty after the resection of osseous tumours, with congenital and post-traumatic craniofacial deformities, requiring reconstructive cranioplasty, and requiring planning of difficult skull base approaches (60). SL models for corrective cranioplasty allowed for the simulation of osteotomies for advancement plasty and craniofacial reassembly in the model before surgery, thus reducing operating time and intraoperative errors. The usefulness of SL models in congenital craniofacial deformities depended directly on the size and configuration of the cranial defect. The indications for the manufacture of individual 3D SL models could be cases of craniofacial dysmorphy that require meticulous preoperative planning and skull base surgery with difficult anatomical and reconstructive problems. The SL models provide 1) a better understanding of the anatomy, 2) presurgical simulation, 3) intraoperative accuracy in the localisation of lesions, 4) accurate fabrication of implants, and 5) improved education of trainees (60). A titanium plate can be customised based on an SL model for ideal adaptation to convex (61, 62), and/or concave skull defects. The reconstruction of unilateral bony defects was also based on the use of virtual mirror imaging of the side controlateral to the side with the defect. An SL mirror model was then produced that served as a template (63) for a cranioplasty implant (64). Finally, implants from diverse sources, such as artificial bone (65), bone allotransfers (66), and titanium mesh (67), were manufactured to fit into cranial defects. An approach combining computer-aided design, SL models and surgical navigation could help manage complex lesions in the skull base and craniofacial area requiring rigid reconstruction (67).

Finally, selectively coloured SL models have been used to construct surgical guides for dental implant placement. The colour allowed for the identification of internal structures, such as the inferior alveolar nerve canal inside the mandible or maxillary sinuses inside the maxilla. It is of major importance when using these RP models to build on surgical guides for implantology (68). SL models have also been used to build surgical guides for zygomatic and pterygoid implants in severely atrophied maxillae (69) and to fix an obturator prosthesis after a large maxillary malignant tumor (46).

Stereolithography accuracy

SL models can provide a highly exact reproduction of the skull in children with craniofacial malformations (70). However, Chang et al. (71) found that the mean differences in the overall dimensions between SL models and skull specimens were 1.5 mm (range: 0-5.5 mm) for craniofacial measures, 1.2 mm (range: 0-4.8 mm) for skull base measures, 1.6 mm (range: 0-5.8 mm) for midface measures, 1.9 mm (range: 0-7.9 mm) for maxilla measures, and 1.5 mm (range: 0-5.7 mm) for orbital measures. The mean differences in defect dimensions were found to be 1.9 mm (range: 0.1-5.7 mm) for unilateral maxillectomy, 0.8 mm (range: 0.2-1.5 mm) for bilateral maxillectomy, and 2.5 mm (range: 0.2-7.0 mm) for orbitomaxillectomy defects. Midface SL models may be more prone to error than those for other craniofacial regions because of the presence of thin walls and small projections. Thus, one should consider designing midface bone replacements that are larger in their critical dimensions than those predicted by preoperative modelling. Choi et al. found that (6) the absolute mean deviation between an original dry skull and an SL RP model over 16 linear measurements was 0.6 +/- 0.35 mm (0.6+/-0.4%). These errors were mainly due to the volume-averaging effect, threshold value, and difficulty in the exact replication of landmark locations. Schicho et al. (72) compared the accuracy of CT and SL models. The accuracy for SL models expressed as the arithmetic mean of the relative deviations ranged from 0.8% to 5.4%, with an overall mean deviation of 2.2%. The mean deviations of the investigated anatomical structures ranged from 0.8 mm to 3.2 mm. An overall mean of deviations (comprising all structures) of 2.5 mm was found. Kragskov et al. (73) also compared the accuracy of CT and SL models and found that the mean difference over all of the investigated cases was 1.9 mm (3.6%). It should also be noted that the limiting factor in SL model accuracy is the imaging technique, rather than the RP technology used. In general, CT and MRI imaging methods acquire image slices that have a slice thickness on the order of 1 to 3 mm, which is much greater than the limiting build resolution of any of the RP technologies (2). In performing a prospective study on the clinical use of SL models, D'Urso et al. (74) concluded that SL models significantly improved operative planning and diagnosis. SL models were found to improve measurement accuracy significantly (image measurement error of 44% compared to biomodel measurement error of 8%, $p < .05$). Surgeons estimated that the use of SL models reduced operating time by average of 17.6% and were cost-effective with a mean price of $1,031 AUS. Patients found SL models to be helpful in the informed consent process. SL modelling is an intuitive, user-friendly technology that has facilitated diagnosis and operative planning. SL models have allowed surgeons to rehearse procedures readily and improved communication between colleagues and patients (74).

Stereolithography artefacts

The CT scanning step is important because the quality of the original CT images directly influences the accuracy of a 3D SL model (6). The 3D image data required for RP models has to follow isotropic multislice CT scanning protocols with a pixel size on the order of 0.5 mm and a slice thickness as low as 1.0 mm (2). The CT scanning step can introduce errors in numerous ways, including with respect to section thickness, pitch, gantry tilt, tube current and voltage, patient movement, metal artefacts of intraoral prostheses, and the slice image construction algorithm itself (6). Due to the nature of the voxel dimension, the reconstruction of 3D models from CT images involves the interpolation of slices to convert the image data volume into an isotropic dataset for mathematical modelling (2). An inherent problem in this computation is that it smoothes out sharp corners or edges between two slices, which is referred to us as the partial volume averaging effect or inter-slice-averaging effect. This effect makes it very difficult to replicate a 3D volume precisely, and because many landmarks are located on sharp vertices or acute edges, the effect may greatly affect the accuracy of 3D models (2). The next step consists of the identification and separation of the anatomical structure of interest (segmentation) for modelling from its surrounding structures, which can be performed by image thresholding, manual editing, or auto-contouring to extract volumes of interest (2). Final delineation of the anatomical structure of interest may require 2D or 3D image editing to remove any unwanted details. A number of software packages are available for data conditioning and image processing for medical RP, including Analyze (Lenexa, KS, www.AnalyzeDirect.com), Mimics by Materialise (Leuven, Belgium, www.materialise.com), and Anatomics (Brisbane, Australia, www.anatomics.net). There remains a need for seamless and inexpensive software that provides a comprehensive range of data interpretation, image processing, and model-building techniques to interface with RP technology (2). The size of 3D models depends on the threshold value, which is a specific density in a slice image that separates the organ of interest and other regions. When the threshold value is specified in a slice, it defines contour lines representing the boundary of the organ of interest. The boundaries obtained from every slice form an iso-surface with the same density. Therefore, it is important to select the proper threshold value (6). The first SL models created were for bone, which was easily segmented in CT image data. Bone has a CT number range from approximately 200 to 2,000. This range is unique to bone within the human body, as it does not numerically overlap with any other tissues (2). All soft tissues outside the threshold range were deleted, leaving only bone structures. Thresholding required the user to determine the CT number value that represented the edge of bone where it interfaces with soft tissue. The choice of threshold may cause a loss of information in areas where only thin bone is present (2). If the bone was particularly thin or the threshold inappropriately measured, a continuous surface was unachievable, leaving the model with a hole where the surface was not closed. In some cases, large areas of bone were removed completely, especially at the back of the orbit and around the zygomatic bone region (partial volume effect) (2). In many circumstances, the volume of the body that is scanned is much larger than that actually required for model construction. To reduce the model size and, therefore the cost, 3D image editing procedures may be employed. The most useful tool for this procedure was a mouse-driven 3D volume editor that enabled the operator to delete or cut out sections from the volume of data. The editing function deleted sections to the full depth of the data volume along the line of sight of the operator. Image editing reduced the overall model size, which also reduced RP building time and costs. Clearer and less complex models may be generated, making structures of interest more clearly visible. Other image processing functions, such as smoothing, volume data mirroring, image addition, and subtraction should be available for the production of models (2). When importing data, the key characteristics that determine the size and scale of the data are the pixel size and the slice thickness (2). The pixel size is calculated by dividing the field of view by the number of pixels. The field of view is a variable set by the radiologist at the time of scanning (2). The number of pixels in the x axis and the y axis is typically 512 x 512 or 1,024 x 1,024. If there is a numerical error in any of these parameters while data are being translated from one data format to another, the model may be inadvertently scaled to an incorrect size (2). The slice thickness (6) and any inter-slice gap must be known (although the inter-slice gap is not applicable in CT imaging, in which images are reconstructed contiguously or overlapping) (2). Numerical error in the slice thickness dimension will lead to inadvertent incorrect scaling in the third dimension. This distance is typically on the order of 1.5 mm but may be as small as 0.5 mm or as great as 5 mm. Smaller scan distances result in higher quality of the 3D reconstruction. The use of the internationally recognised DICOM (Digital Image Communications in Medicine) standard for the format of medical images has largely eliminated these errors (2). Additional sources of error in 3D model reconstruction include topological defects, such as tessellation, triangle edge, and closure errors, the decimation ratio for surface smoothing, and the methods of interpolation used. The RP manufacturers that provide 3D reconstruction software are concerned with the ability to deal with topological incompleteness and surface smoothness. Errors can arise during the actual production and curing of RP models, including errors associated with the residual polymerisation and transformation of RP materials, the creation and removal of support structures (to avoid unsupported or weakly supported structures), laser diameter, laser path, thickness of layers, and finishing (6). Model stair-step artefacts represent the stepped effect seen in medical models. One contribution to these artefacts comes from the discrete layer thickness at which the model is built, which is a characteristic of the particular RP process and material being used. Typically, these thickness range from 0.1 mm to 0.3 mm. This effect can be minimised by selecting processes and parameters that minimise the build layer thickness. However, thinner layers result in longer build- times and increased costs, and an economic compromise is typically found for each RP process. As the layer thickness is typically an order of magnitude smaller than the slice thickness of the CT images, it does not have an overriding effect on the quality of the model. The second effect arises from the slice thickness of the acquired CT or MR images and any potential gap between them (2). Both SL and fusion deposing modelling (FDM) required support structures during the build process. These are subsequently cleaned from the model manually, although they generally leave a rough surface, which does not affect the overall accuracy of the model but contributes to a degradation of its aesthetic appearance. It is unlikely that these structures will have a detrimental effect on surgical planning or implant design (2). The mathematical modelling of a surface will introduce its own surface effects. The smoothness (governed by the size of the triangle mesh) of the model surface becomes poorer as the surface mesh becomes larger. A larger mesh results in a lower number of triangles, reduced computer file size, and faster rendering. A smaller mesh results in a much better surface representation, much greater computer file size, and slower rendering (2).

Stereolithography: conclusions

Complex surgical procedures, especially those related to craniofacial structures, appear to benefit significantly from the preplanning and implant construction allowed by physical prototypes. It has been hypothesised that the costs of RP are offset by associated reductions in the number of inaccurate and incomplete complex surgical procedures. The costs of revision procedures and for the replacement of ill-fitting custom implants (which can cost up to $3,000) are significant compared with the cost of applying a centralised rapid medical prototyping service (1, 75). Many advantages of SL models have been identified: 1) the quality of preoperative planning is greatly improved by allowing a better understanding of the anatomy, and the extent of the disease, 2) the best approach to an osteotomy, and, to the associated surgical site can be assessed, and a more realistic simulation of the surgical steps can be conducted, 3) SL medical models provide an excellent reference when discussing surgical procedures with patients, thus enhancing the validity of informed consent, as the patients gain a greater understanding of the technical difficulties and limitations of the proposed surgery, 4) medical training and surgical education can be undertaken, away from already overcrowded surgical suites, and communication between different specialties allows for a more comprehensive multidisciplinary approach (75), 5) the predicting of results improves with more accurate custom implant manufacturing, pre-planned screw placement, and osteotomy design, which also reduces operative time (76-78).

SL models can also be sterilized and used directly in the operating theatre. The disadvantages of this technique are mainly those inherent in MRI and CT imaging. Additionally, only one model per simulation can be used, and storage areas will be needed with intense use of these biomodels (79). Furthermore, the necessary equipment for producing these models is quite costly, and the cost of the fabrication of a composite skull model is presently and is likely to remain very expensive. Although the use of SL models in routine cases is quite rare, they are already in use at various universities and institutions with very satisfactory results, especially in severe cases of maxillofacial deformities (3). Finally, the limitations of the SL modelling technique include a lengthy production time which renders it unsuitable for emergency cases, and radiation exposure of the patient. With wider use and further technological development, these drawbacks will be minimised. In the future, 3D SL biomodels may become an adjunct not only to maxillofacial surgery but also to other medical specialties (80).

SELECTIVE LASER SINTERING (SLS)

Selective laser sintering: clinical applications

SLS model has been used in the presurgical planning for a tumor surgery to assist with mandibular reconstruction using fibular grafts after ameloblastoma resection (81). Before surgery, the surgeon used the initial SLS biomodel with the tumour to mark the areas where osteotomies should be performed and to determine the shape and magnitude of an autogenous graft implant. An SLS model could also be used during surgery as a guide for the surgeon to mark the bone graft taken from the fibula and transfer the position of osteotomies from the SLS preoperative model to the operating theatre (81). A custom-made SLS model has also been developed that can be fitted at any site of a microvascular fibula flap, taking into account the vascular anatomy (82). This procedure enhanced the visualisation of points to be remodelled in an autogenous fibular graft to reproduce a new mandible (81). The accuracy of SLS model is relatively high with standard errors of a maximum of 0.1 to 0.6 mm. This accuracy depends on the thickness of the CT scans used, which should be as thin as possible (1 to 2 mm is a good compromise for a skull study); the field of view should have a resolution of 512 x 512 and not generate tilting during image acquisition (82).

Relying on the accuracy of the guide, osteotomies and plating can be safely and swiftly performed with the osseous flap in place, which reduces the ischemic time. Having access to a virtual plan preoperatively allows a surgical team to discuss a procedure in detail, and surgeons can improve or refine treatment plans and produce custom-made devices in advance. Such virtual plans allow for the movement of bony segments to find the best positions with regard to function, aesthetics and blood supply (the vascular anatomy can be visualised), which means that the optimal donor location on the fibula can be determined. Using RP model to manufacture a guide directly from a dataset obtained from the virtual plan eliminates the intermediate steps of model construction, from which different types of guides are produced (82).

A 3D SLS skull model has been found to be able to accurately reproduce and reconstruct a fracture model (83) and fully reveal the anatomical structure of the craniomaxillary bone and its relationship to surrounding tissues. It has been used to mimic surgeries for repairing CMF trauma, to determine the validity of a surgical design, to predict surgical outcomes, to weigh various approaches, to determine an intraoperative guiding template, and to shorten operation time and minimise surgical risks (84). The advantage of SLS technology over SL is that it produces models with higher accuracy. This accuracy is especially important in reproducing thin osseous structures of fractured orbital floors for the purpose of manufacturing new custom-made titanium orbital floors (85). An SLS polyamide model has been used for repairing large skull defects by constructing custom-made cranial plates. Custom-made cranioplasty implants are associated with the advantages of reduced operative time, less invasive surgery, improved cosmetic results, faster recuperation, and reduced costs due to shorter operative times (86). SLS models have also allowed for the analysis of abnormalities regarding calvaria morphology, nasal bones and maxilla, improving the criteria for diagnosis and the surgical plan in a case of craniofacial dysostosis (Apert syndrome) (87, 88). Finally SLS model was used for surgical preoperative planning in TMJ ankylosis (87).

Selective laser sintering accuracy

The accuracy of the SLS model is relatively high, with maximum standard errors of 0.1 to 0.6 mm. This accuracy depends on the thickness of the CT scans used, which should be as thin as possible (1 to 2 mm is a good compromise for a skull study); the field of view should have a resolution of 512 x 512 and not generate tilting during image acquisition (81). Silva et al. (89) and Ibrahim et al. (90) found a dimensional error of 2.1% for the SLS prototype in comparison with the dry skull. The authors found an inverse correlation between the external and internal dimensions that may be explained by the dumb-bell effect described by Choi et al. (6), in which an increase in external dimensions and a simultaneous decrease in internal dimensions indicated that the prototypes had larger dimensions than the original skull and that the selected threshold may have been too low. Therefore, accuracy is dependent primarily on the choice of scanning protocol, on data segmentation and, especially, on the determination of the threshold. One factor that may partially explain the smaller dimensions of SLS prototypes is the superficial wear caused by sandblasting (89). The unused powder that surrounds the prototype in the SLS system cannot be reused. Because of the high cost of the material, several parts are fabricated simultaneously. The long fabrication time for the SLS technique (16 hours) is very close to the time required for fabrication with the SL system (89).

FUSED DEPOSITION MODELLING (FDM)

Fused deposition modelling: clinical applications

Fused deposition modelling (FDM) uses a similar principle as SL in that it builds models on a layer-by-layer basis. The main difference is that the layers are deposited as a thermoplastic that is extruded from a fine nozzle. In this systematic review, we found that only a surgical template for dental implant drilling had thus far been developed based on this technique (91).

THREE-DIMENSIONAL PRINTING (3DP)

Three-dimensional printing: clinical applications

A 3DP model has been used for repairing orbital floor fractures using pre-shaped titanium mesh implants formed based on anatomical 3DP models of the orbit (92). The unaffected orbit was mirrored onto the contralateral side, i.e., the injured orbit. This model contained numerous artefacts, which is typical of CT studies because of the very thin bone structures of the orbit. To create a rigid physical model that will be strong enough to be used as a template, all of the empty spaces (air) surrounding the mirrored orbit in the virtual model were filled in, which resulted in a virtual model of the orbit that was surrounded only by hard tissue (92, 93). Next, the virtual model data were converted to an STL format, and solid physical models were created from acrylic resin using a 3D printer. The resulting physical models were stronger and more rigid than if they had been built containing hollow structures i.e., maxillary and ethmoid sinuses (92). The use of 3DP models in orbital floor reconstruction has numerous advantages, such as the following (92): 1) increasing the understanding of orbital disruption; 2) shortening the operation time; 3) decreasing the number of attempts at positioning an implant in the orbit and verifying the shape and fit; 4) serving as a guide for the surgeon during surgery; 5) being relatively inexpensive. However, this method is also associated with some disadvantages, such as the following: 1) the length of time required to build model; 2) the cooperation required between a number of people in different locations; and 3) the use of this method in panfacial fractures is challenging because it is difficult to find any stable orbital margins for virtual planning of the model and to establish an accurate position for the pre-shaped plates (92).

Preoperative orthognathic surgery plans can be tested using 3DP models. The relationship between proximal and distal mandibular segments after bilateral sagittal split osteotomies has been evaluated on models preoperatively. Studying the planned movements of osteotomised bone segments preoperatively and observing the relationships of osteotomised segments of the mandibula and maxilla in orthognathic surgery increased the intraoperative accuracy (94). A 3DP multi-position model was also used to prebend titanium plates and produce a surgical guide for transferring osteotomies from the 3DP model to the operating theatre in genioplasty (95). Additionally, 3DP models have been used for planning distraction osteogenesis related to complex craniofacial malformations (osteotomies, vector of distraction). The customised fixation plates of a distractor, primarily prepared on the 3DP model, can be easily adapted during surgery to predicted positions due to their high accuracy of fit. These customized plates enable the parallel alignment of both connecting pins, which ensures the proper transmission of distraction forces to the mobilised segment

(96). Furthermore, 3DP models have been used in mandibular resection and reconstruction using a reconstructive plate (54). The plate was precontoured according to the 3DP model. Precise adaptation of the plate and excellent symmetry were achieved within a relatively short operation time. Plate handling in the operating theatre was minimal, thus preserving its strength. Other benefits of using 3DP models include decreased exposure time to general anaesthesia, decreased blood loss and shorter wound exposure time. The advantages of 3DP model techniques include the special understanding of bone morphology that is provided, accurate and easier planning of preoperative plate bending, and much more accurate bone harvesting due to using the negative imprint of the gap to be reconstructed. Thus, 3DP technology is a reliable method for assisting in precise mandibular reconstruction using bone plates and bone grafts. Compared with other 3D methods, this method can be performed more quickly and easily and is more cost-effective. Furthermore, it is superior in printing smaller and more complex structures (48).

Three-dimensional printing: accuracy

Silva et al. (89) reported a mean dimensional error of 2.7% in prototypes produced using 3DP technologies in comparison with a dry human skull (criterion standard). In the 3DP system, the printing mechanism, the type and quality of the materials used in the fabrication of the prototypes (powder), and the absorption properties of the powder when in contact with the binder and infiltration material (to increase the strength of 3D model) are parameters that should be controlled to obtain a reliable final product. It is possible that the 3DP prototypes were larger than the dry skulls because of cyanoacrylate infiltration. The powder remaining in the 3DP system may be reused, and the parts may be fabricated individually, which substantially reduces prototype fabrication time (4 hours). Therefore, the 3DP technique has a lower final cost than the SLS technique, which, in turn, has a lower cost than the SL technique (89). Advantages of 3DP over SLS include a faster printing time and lower costs (48). However, SLS prototypes have a better dimensional precision and reproduce anatomical details of the craniomaxillary region more accurately than 3DP prototypes (89). Ibrahim et al. obtained a dimensional error for 3DP of 1 mm (2.7%) when comparing SLS (0.9 mm and 2.1%) and 3DP models and dry skulls (90).

POLYJET MODELLING

Polyjet modelling is performed by jetting state-of-the-art photopolymer materials in ultra-thin layers (16 µm) onto a build tray layer by layer until the model is completed. At present, this technique is too time-consuming and, therefore, too expensive to be used in CMF surgery clinical applications. Ibrahim et al. (90) reported a dimensional error of 2.1% in reproducing a dry mandible when using this technique.

NEW CLINICAL APPLICATIONS OF RAPID PROTOTYPING MODELS IN CRANIO-MAXILLOFACIAL SURGERY

Three-dimensional rapid prototyping model, modelling clay, surgical guide, and pre-bent titanium mesh in reconstruction of the posttraumatic orbital floor.

Introduction

Different methods, surgical approaches, and materials (92, 97) were proposed for reconstruction of the posttraumatic orbital floor. Recently, the use of 3D pre-bent titanium implants in a 3D RP model was introduced (92). However, even if the pre-bent titanium mesh fits perfectly on the 3D RP model, transfer of the pre-bent mesh from the 3D RP model to the operating room while maintaining exact an position remains challenging. Therefore, we present a method that involves the use of a RP model-based prefabricated surgical drill guide to improve the pre-bent titanium mesh positioning.

Case report

A 38-year-old male patient presented to our Department of Oral and Maxillofacial Surgery three weeks after facial trauma occurred during his weekly boxing course. Anamnesis revealed a period of extensive left periorbital swelling immediately following the injury. However, no medical consultation was performed at that time. The clinical examination revealed a left eye enophthalmos and an upgaze diplopia. The patient also presented a hypoesthesia of the left infra-orbital nerve. The patient's main concern was esthetic, related to the accentuated palpebral fold on the left side. A low-dose CT scan was performed (98). The patient presented with a combined maxillofacial fracture of the left orbital floor, the left anterior maxillary sinus wall and the nasal bones (Fig. 1. A, B).

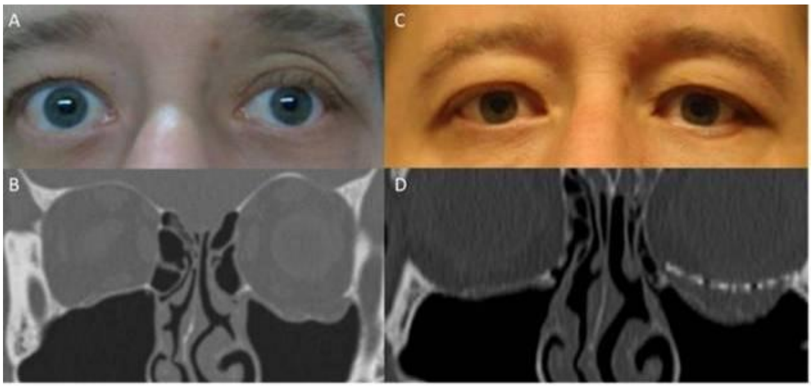

Figure 1. (A) Pre-operative appearance of the face, accentuated palpebral fold on the left side; (B) Preoperative low-dose CT scan, coronal view; (C) Postoperative appearance of the face, correction of the left palpebral fold; (D) Postoperative low-dose CT scan, coronal view, restoratio ad integrum of the inferior left orbital wall with the pre-shaped titanium mesh.

Method

A 3D RP model (Z Corp, Burlington, USA) was created based on low-dose CT data (DICOM files, STL format) (98). We used modelling clay (Décor fin, Royal Talens, Holland) to fill in all the holes of the orbital floor on the 3D RP model. The modeling clay also served to reconstruct the left orbital floor such that it was symmetric to the right side. Then, a sheet of paper was cut to fit in the left orbital floor. A titanium mesh (0.4 -mm in width) was then cut from a 100 x 100 -mm titanium mesh plate (Synthes, Oberdorf, Switzerland) with a sheet of paper as a guide. The titanium mesh was then appliedand pre-bent on the 3D RP model. The holes for the screws were marked with a pencil on the anterior orbital rim of the 3D RP model (Fig. 2. A). The acrylic guide for positioning the screws was prepared according to the shape of the left orbital rim. Aluminum cylinders were inserted into the acrylic surgical guide to guide the 1.8 -mm diameter drill. The aluminum cylinders were inserted perpendicular to the underlying bone surface (Fig. 2. B). The pre-bent titanium mesh and the acrylic guide were sterilized using a standard procedure. The fracture site was exposed with the patient under general anaesthesia, via a subciliary approach to the left orbital floor. The herniated fat and muscle tissue were moved up to avoid further necrosis and to increase the intra-orbital volume. The prefabricated surgical acrylic guide was inserted in the inferior left orbital rim (Fig. 2. C). Four holes were drilled in the left orbital rim, through the guide, using an 8 -mm drill. The pre-bent titanium mesh was then positioned in the orbit and fixed to the inferior orbital rim by means of three 4 -mm screws and one 6 -mm screw. The diameter of each screw was 1.8 -mm (Fig. 2. D). Clinical postoperative follow-ups at one week and one month showed no diplopia and correction of the palpebral fold. Radiological follow-up revealed a restitutio ad integrum of the left orbital floor (Fig. 1. C, D).

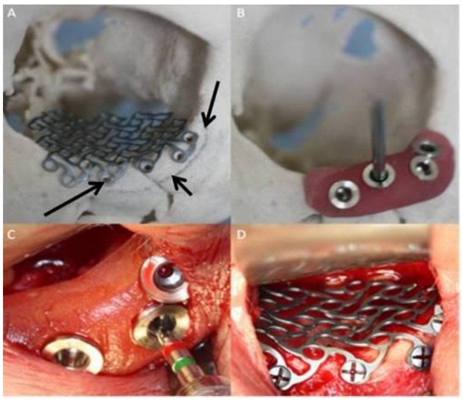

Figure 2. (A) Pre-bent titanium mesh on the three-dimensional rapid prototyping (3D RP) model, with holes for screws and size of the guide marked with black pencil on the 3D RP model (arrows); (B) Acrylic surgical guide for positioning the holes for screws on the 3D RP model, positioning of the drill at 90° in relation to the bone surface; (C) Intra-operative drilling of holes through the surgical guide; (D) Intra-operative view of the positioning of the pre-bent titanium mesh on the left orbital floor.

Discussion

The recently presented use of pre-bent titanium mesh in 3D RP models (92, 99) allows for accurate repositioning of a de novo reconstructed orbital floor. However, there are multiple alternative positions for insertion and positioning of the pre-bent titanium mesh inside the orbit. This is especially true for medio-lateral positioning of the titanium mesh, due to relative lack of precise anatomical landmarks on the inferior orbital rim. The acrylic surgical guide allows for transfer of holes for screws from the position appropriate for 3D RP planning to that used in the operating theater (95).Therefore, there exists only one 3D position for the pre-bent titanium mesh inside the orbit. This cost-effective method could also be an alternative to most cost- and time- consuming navigation-based methods (100, 101). To pre-bend the intra-orbital part of the titanium mesh a 3D virtual model of the orbit was described and constructed as a 3D RP model (92). The 3D virtual model required two steps: 1) a mirroring of the right side of the orbital floor on the left side and, 2) a virtual filling in all the empty virtual spaces present because of partial volume effect and of true spaces, that are anatomically present. All these steps were time-consuming and necessitated an experienced engineering team (92). The use of the modelling clay directly on the 3D RP model precludes the need for time-consuming, complex computer-assisted manipulations, knowledge of advanced software, or an engineering team. Finally, the use of a sheet of paper allows economical use of 100 x 100 -mm mesh titanium plates.

Innovative procedure for computer-assisted genioplasty: three-dimensional cephalometry, rapid prototyping model and surgical splint (95).

Introduction

Genioplasty plays an important role in harmonizing facial proportions and profiles. However, planning a genioplasty remains a difficult task because of limited means of diagnosis, planning and information transfer to the operating room. Specifically, the theoretical virtual anteroposterior and vertical positions of the chin are reduced to the landmarks “menton”, “B point”, and “pogonion” on two-dimensional cephalograms (102). We propose and describe the combined use of 3D cephalometry, a 3D rapid prototyping model, and pre-bent titanium plates as a new means of computer-assisted genioplasty.

Method

A young adult patient presented in our clinics after an orthodontic treatment was completed elsewhere. At clinical examination, the patient still presented a retrusive profile and refused any orthognathic treatment for the occlusion (Fig. 3. A). Therefore, we proposed an advancement genioplasty. We received approval from the local ethics committee (B40320084307) for the clinical

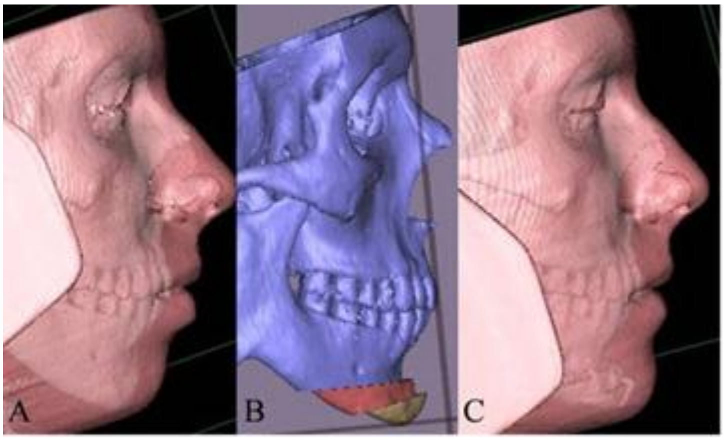

Figure 3. (A) Pre-operative profile; (B) Virtual planning, double advancement of the chin; (C) Post-operative profile. This figure was originally published in *Int J Oral Maxillofac Surg*. Olszewski R, Tranduy K, Reychler H. Innovative procedure for computer-assisted genioplasty: three-dimensional cephalometry, rapid prototyping model and surgical splint. *Int J Oral Maxillofac Surg*. 2010;39(7):721-724. Copyright © 2010, Elsevier.

application of the 3D cephalometric analysis, and the subject gave informed consent for the study.

A low-dose CT scan of the head was performed (98) from which we determined the anterior, posterior, and inferior limits of the chin with the newly-developed and validated 3D cephalometric planar analysis (ACRO 3D) (Fig. 3. B) (98, 103). The osteotomy lines were planned and visualized with Mimics software (Materialize, Leuven, Belgium). We positioned the upper osteotomy line at a distance of at least 5 mm from both mental foramina. The amount of movement was virtually planned with Mimics software in relation to the reference planes from the ACRO 3D analysis (Fig. 3. B). We then built a 3D RP model from the low-dose CT scan with a 3D printer (Z-Corp, Burlington, USA) (89). The 3D RP model was presented as a multi-position 3D model (Fig. 4.) with initial, intermediary, and final positions of the bony slices of the chin.

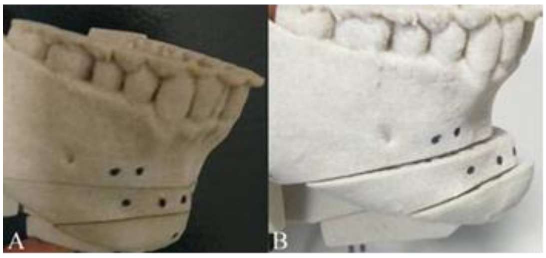

Figure 4. (A) Pre-operative initial position of chin bone segments; (B) Postoperative final position of chin bone segments. Black dots indicate the position of holes for the screws. This figure was originally published in Int J Oral Maxillofac Surg. Olszewski R, Tranduy K, Reychler H. Innovative procedure for computer-assisted genioplasty: three-dimensional cephalometry, rapid prototyping model and surgical splint. Int J Oral Maxillofac Surg. 2010;39(7):721-724. Copyright © 2010, Elsevier

We used the final position of the 3D RP model to pre-bend the titanium plates and to indicate the positions of the holes for screws corresponding to the pre-bent plates. The 3D RP model was then repositioned to its initial position and an acrylic surgical guide was made. The role of the surgical guide was to transfer the position of the holes for the screws (in their final position) and the osteotomy lines. The surgical guide was sterilized at 120° Celcius for 20 minutes in an autoclave. The pre-bent titanium plates were also sterilized (92). During the surgery and before the osteotomy, the acrylic guide was positioned on the osseous chin of the patient. First, we drilled the holes for the screws through the surgical guide (Fig. 5.). Then, with a sterilized pencil (104) we drew the osteotomy lines based upon the surgical guide (Fig. 5.).

Osteotomy cuts were performed following the pencil tracings. Finally, after complete separation of the bony fragments, we positioned and screwed the pre-bent plates (Fig. 6.). A low-dose CT scan showed a good result in the patient's profile (Fig. 3. C).

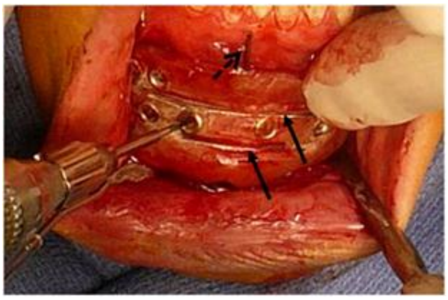

Figure 5. Acrylic guide positioned on the osseous chin of the patient. Holes for the screws drilled through the surgical guide. Plain arrows showing transfer lines for osteotomy paths. Broken arrow shows the midline indicator of the acrylic guide. This figure was originally published in Int J Oral Maxillofac Surg. Olszewski R, Tranduy K, Reychler H. Innovative procedure for computer-assisted genioplasty: three-dimensional cephalometry, rapid prototyping model and surgical splint. Int J Oral Maxillofac Surg. 2010;39(7):721-724. Copyright © 2010, Elsevier

Figure. 6. Positioning and screwing of the pre-bent plates. This figure was originally published in Int J Oral Maxillofac Surg. Olszewski R, Tranduy K, Reychler H. Innovative procedure for computer-assisted genioplasty: three-dimensional cephalometry, rapid prototyping model and surgical splint. Int J Oral Maxillofac Surg. 2010;39(7):721-724. Copyright © 2010, Elsevier

Discussion

Computer-assisted genioplasty seems to be the next step in the evolution of computer-assisted orthognathic surgery (105). The combination of different 3D methods for the diagnosis (3D cephalometric analysis), virtual planning (Mimics software), and transfer (3D RP model, surgical guide, and pre-bent plates) allowed for a complete 3D treatment of this case. The 3D cephalometry plays an important role in planning a genioplasty. For the first time, the chin region was evaluated with more than a single landmark ("menton", or "pogonion") as is normally the case with 2D cephalometrics (102). We have limited the presentation of the 3D cephalometry in Fig. 3. B to the region of interest, which was the evaluation of the chin. The concept, software, and experimental validation of the 3D cephalometric planar analysis have been previously published (103). Three planes (anterior, posterior and inferior) determine the theoretically ideal and individual position for the osseous chin volume in the 3D space. However, the final decision for the position of the chin must also involve consideration of the soft tissue in the patient's profile. The position of the chin is dependent on the desires of the patient and on the clinical judgment of the surgeon. Therefore, there can be a discrepancy between the conclusions of the theoretical 3D cephalometry and the clinical experience. In this case, the final amount of bone movement in the anteroposterior direction was inferior to that proposed by the 3D cephalometric analysis (anterior plane). It must be stressed that the visualization of soft tissues in Fig. 3. (A-preoperative) and (C-postoperative) represents the true soft-tissue profile of the patient pre- and post-operatively. Virtual planning showed that there was only a place for one screw on the lower part of the chin osteotomy. With the virtual planning we decided preoperatively on the best positioning for that screw. The stability of the lower part of chin osteotomy was also achieved with a pre-bent plate formed on the 3D RP model. Virtual planning allows for the visualization of the roots and for better positioning of the screws in relation to the roots. For that reason, the chance of root damage is very low in comparison to techniques without a computer-generated surgical splint. The 3D RP model allowed for a transfer of parallel osteotomy lines to the operating room. We also were able to propose a sandwich technique, which allowed for the following: 1) a bigger advancement compared to one-piece movement, and 2) improved stability and healing of the displaced bony slices. The use of the sterilized computer-generated surgical guide and pencil was also cost-effective compared to currently available navigation systems (106). We modified the use of the 3D RP model from a diagnosis-only purpose (107) to making a transfer of virtual information to the operating room. It should be stressed that building a 3D RP model with 3D printers is now more affordable (less than 300 Euros for a 3D RP model) than stereolithographic models (92). Also, the time spent on the osteotomy and on bending plates was decreased during surgery. The possible chin drop related to increased muscle detachment in the sandwich technique was avoided due to mental muscle reattachment at the end of the surgery. The postoperative results of the new technique are promising. The technique is fast and is easy-to-use due to its computer-generated surgical splint and pre-bent plates. More patients are needed for definitive clinical validation of this procedure. Of note, the same approach of combining 3D cephalometric analysis, 3D multi-position RP models, surgical cost-effective computer-generated surgical guides and pre-bent plates may be of interest in other orthognathic surgery.

New three-dimensional (3D) surgical guide for frontal-nasal-ethmoid-vomer osteotomy (108)

Introduction

Lefort III surgery is a classical surgery performed to correct craniofacial craniosynostoses (109). The majority of the osteotomy lines are performed through via open sky access or with the tactile contact (pterygopalatine disjunction with an Obwegeser osteotome). However, frontal-nasal-ethmoid-vomer osteotomy is performed in a blind manner based only on the experience of the surgeon. The main risks during this type of osteotomy are linked to the initial wrong 3D orientation of the osteotome in relation to the patient's anatomy. The anatomy of a craniosynostotic syndromic patient could also be misleading for initial orientation of the osteotome (88). An osteotomy performed in too anterior and/or too lateral a direction could result in a bad split of the midline during the down-fracture with Rowe forceps. If performed in too posterior a direction, the ethmoid body could be entered, resulting in intense bleeding and olfactive nerve damage. Finally the depth of insertion of the osteotome in relation to the frontonasal suture is also an issue: too short an insertion will result in incomplete midfacial disjunction and uncontrolled midfacial fracture during the down-fracture with Rowe forceps. Therefore, we propose a new technique based on a 3D surgical guide for frontal-nasal-ethmoid-vomer osteotomy based on a 3D rapid prototyping model. The method was applied to a 7-year- old Apert craniosynostosis patient. Lefort III osteotomies were associated with internal distraction devices for the midface advancement (110).

Material and Methods

A 3D CT of the skull was acquired in a standard head position with a previously validated low- dose CT protocol (98). The protocol dictates a 1mm slice, with 512x512 matrix, 210 mm field of view, 120 kV and 42 mA. The native data were saved on a CD (DICOM format). The 3D CT reconstruction was performed by Mimics software (Materialize, Leuven, Belgium) and saved under STL format. A RP model of the skull was obtained with a 3D printer (Z Corp, Burlington, USA). We drilled a groove in the nasal bones until the frontal-nasal suture was reached. A osteotome of 5 mm width was positioned inside the nasal fossa, with anterior-posterior orientation, from the nasal-frontal suture toward the level of posterior nasal spine. Following this, PMMA resin (Palacos, Heraeus Medical, Germany) was moulded around the osteotome and around the nasal bones (Fig. 7., Fig. 8.).

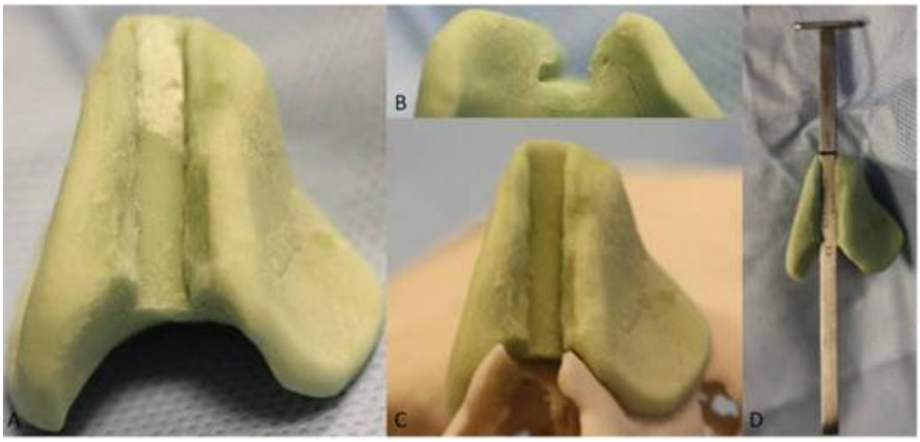

Figure 7. (A) Anterior view of customized 3D osteotomy guide in PMMA resin; (B) Inferior view of the 3D guide: the groove for osteotome; (C) Anterior view: positioning of the 3D guide on the 3D RP model; (D) Anterior view: checking the sliding movement of the osteotome through the 3D guide. The final depth to insert the osteotome is indicated with alcohol pen. This figure was originally published in J Craniofac Surg. Olszewski R, Reychler H. Three-dimensional surgical guide for frontal-nasal-ethmoid-vomer disjunction in le fort III osteotomy. J Craniofac Surg. 2011;22(5):1791-1792. Copyright © 2011, Lippincott, Williams & Wilkins

Figure 8. (A) Positioning of the 3D guide, and osteotome on the patient's 3D RP skull model; (B) Superior view: checking the insertion of the osteotome inside the 3D guide; (C) Inferior view: checking the posterior limit of the osteotomy at the level of posterior nasal spine. After the thermo-reaction ended, the 3D guide was polished with dental burrs and sterilized in an autoclave under standard conditions (135° Celcius, 20 minutes). The distance from the top of the 3D guide and the posterior nasal spine was also measured on the 3D RP model (8.3 cm). This figure was originally published in J Craniofac Surg. Olszewski R, Reychler H. Three-dimensional surgical guide for frontal-nasal-ethmoid-vomer disjunction in le fort III osteotomy. J Craniofac Surg. 2011;22(5):1791-1792. Copyright © 2011, Lippincott, Williams & Wilkins

Results

The surgery was then performed classically with bi-coronal and intraoral accesses. All Lefort III osteotomies were performed classically with drills and osteotomes. The 3D guide was positioned on the top of the frontal-nasal sutures. No cranial pressure was induced with the 3D guide at any time during the procedure. We used an osteotome of 5 mm width. We marked a reported distance from the 3D RP model (Fig. 8. A) on the osteotome with an alcohol pen (Fig. 9., arrow). The osteotome was then positioned in the flat groove inside the 3D guide and inserted into the bone with the orientation provided by the 3D guide until it reached the marked depth (at the level of posterior nasal spine) (Fig. 9., arrow).

Discussion

Performing frontal-nasal-ethmoid-vomer osteotomy seems to be one of critical issues in Lefort III surgery (111, 112). Therefore, every technique facilitating this procedure could immediately help the surgeon and protect the patient from major complications. We presented a technical approach based on the optimization of the use of 3D RP models. 3D RP models are mainly used for diagnostic purposes (107). However, 3D RP models allow also for the transfer of 3D data from planning to the operating theatre (92). We used a 3D printer technique (Z Corp, Burlington, USA) to build a 3D RP model of the skull (92). The 3D printed models have an economical advantage over stereolithography and retain the accuracy

Figure 9. Intra-operative view. Insertion of the osteotome with the 3D guide trough the nasal bones (dashed arrow) until reaching the predicted depth (arrow shows a mark on osteotom). On the right, orbitofrontal bandeau is deposed at that time of surgery, and compresses cover the brain (*). On the left, bicoronal flap raised up at the beginning of the surgery. This figure was originally published in J Craniofac Surg. Olszewski R, Reychler H. Three-dimensional surgical guide for frontal-nasal-ethmoid-vomer disjunction in le fort III osteotomy. J Craniofac Surg. 2011;22(5):1791-1792. Copyright © 2011, Lippincott, Williams & Wilkins

required for medical modelling (90). The PMMA resin (Palacos, Heraeus Medical, Germany) was used to create the 3D guide.This material is easy to use, cost - effective, and allows for fast 3D moulding of the frontal-nasal area. The positioning of the 3D guide on the patient does not require a supplementary task by the surgeon, such as registration and tracking in intra-operative navigation (113). The individualized 3D guide allows three main pieces of information to be transferred from the 3D RP model: impact point for the osteotome, orientation in the 3D space, and the depth for the insertion of the osteotome. This technique allows a critical osteotomy path in Lefort III surgery to be transferred in a secure, fast, and cost-effective manner from the 3D RP model to the operating room. Further study will consists in verification of the accuracy of using customized 3D guides for subcranial separation of the face at the nasofrontal region on cadavers.

CONCLUSIONS AND FUTURE DIRECTIONS

Three-dimensional RP models are used in association with a variety of applications in CMF surgery. These techniques need still a close collaboration between clinicians and engineers with specific expertise (1). Also there is still room for innovation and for new uses related to additional indications. However, randomized control trials should be developed to prove the real usefulness of 3D RP models in CMF surgery. Moreover, increasing the accuracy of RP techniques is still required but without supplementary irradiation of the patient. For this reason, attention should focused on the implementation of low-dose CT scans and cone beam CT scan protocols for data acquisition. Additionally, an effort should be made to develop 3D RP models from alternative image sources, such as MRI, ultrasounds, and laser scan imaging. More cost-effective methods are required for the broad application of these modeling technique beyond the most developed countries. For this reason, 3DP technique appears be more realistic for current clinical use than SL or SLS techniques. Other cost-effective RP techniques, such as 3D paper printing (http://www.mcortechnologies.com), should also be investigated in terms of accuracy and applicability and, to increase the availability of 3D RP technology to CMF surgeons and to improve patient care (Fig. 10.).

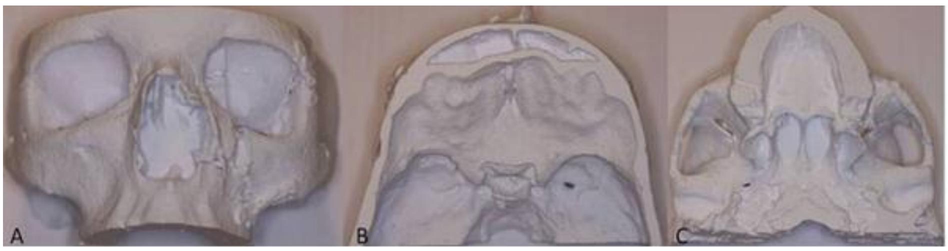

Fig. 10. Three-dimensional paper printed skull model. (A) Frontal view; (B) Endocranial view; (C) Inferior view.

Such 3D RP models should be used not only for diagnostic purposes but also mainly for transferring virtual plans to the operating theatre. In this process, 3D RP models should be competitive against computer-assisted navigation techniques, which are accurate but still very expensive and time-consuming. Another important factor related to the use of these models is the time required for their fabrication, which should be shortened to allow the use 3D RP techniques directly in emergency rooms to enlarge the field of potential indications they may be used to address. Finally, CMF surgery might profit from the most advanced and emerging 3D printing techniques, such as organ printing (114). Organ printing is a biomedically relevant variant of RP technology, which is based on tissue fluidity. Computer-assisted deposition (printing) of natural materials (cells or matrices) is performed one layer at a time until a particular 3D form is achieved (115). However, recent attempts using RP technologies to design solid synthetic scaffolds (114) suffered from an inability to precisely place cells or cell aggregates into a printed scaffold. Thus, organ-printing technology will become increasingly more secondum naturam. Mironov et al., (116, 117) defined organ printing as a RP computer-aided 3D printing technology based on using the layer-by-layer deposition of cells and/or cell aggregates into a 3D gel, with the subsequent maturation of the printed construct in perfused and vascularised living tissues or organs. This definition of organ printing includes the many different printer designs and components associated with the deposition process that are currently available, such as jet-based cell printers, cell dispensers or bioplotters, different types of 3D hydrogels and varying cell types. Such computer-assisted tissue engineering using 3D live RP technology will certainly open a new era for reconstructive CMF surgery.

Acknowledgements

The author would like to thank the Royal Academy of Medicine of Belgium for receiving the annual award Jeanne et Marie François 2011 for the memory: “Three-dimensional rapid prototyping models in cranio-maxillofacial surgery: systematic review and new clinical applications”.

LIST OF REFERENCES

1. Sugar A, Bibb R, Morris C, Parkhouse J. The development of a collaborative medical modelling service: organisational and technical considerations. Br J Oral Maxillofac Surg 2004 Aug;42(4):323-330.
2. Winder J, Bibb R. Medical rapid prototyping technologies: state of the art and current limitations for application in oral and maxillofacial surgery. J Oral Maxillofac Surg 2005 Jul;63(7):1006-1015.
3. Mankovich NJ, Samson D, Pratt W, Lew D, Beumer J 3rd. Surgical planning using three-dimensional imaging and computer modeling. Otolaryngol Clin North Am 1994 Oct;27(5):875-889.
4. Edwards SP. Computer-assisted craniomaxillo-facial surgery. Oral Maxillofac Surg Clin North Am 2010 Feb;22:117-134.
5. Ono I, Gunji H, Suda K, Kaneko F. Method for preparing an exact size model using helical volume scan computed tomography. Plast Reconstr Surg 1994 Jun;93(7):1363-1371.
6. Choi JY, Choi JH, Kim NK, Kim Y, Lee JK, Kim MK, Lee JH, Kim MJ. Analysis of errors in medical rapid prototyping models. Int J Oral Maxillofac Surg 2002 Feb;31(1):23-32.
7. Papadopoulos MA, Christou PK, Christou PK, Athanasiou AE, Boettcher P, Zeilhofer HF, Sader R, Papadopulos NA. Three-dimensional craniofacial reconstruction imaging. Oral Surg Oral Med Oral Pathol Oral Radiol Endod 2002 Apr;93(4):382-393.
8. Sato K, Sugawara J, Mitani H, Kawamura H. Use of selectively colored stereolithography for diagnosis of impacted supernumerary teeth for a patient with cleidocranial dysplasia. Int J Adult Orthodon Orthognath Surg 1998;13(2):163-167.
9. Westendorff C, Kaminsky J, Ernemann U, Reinert S, Hoffmann J. Image-guided sphenoid wing meningioma resection and simultaneous computer-assisted cranio-orbital reconstruction: technical case report. Neurosurgery 2007 Feb;60(2 Suppl 1):ONSE173-174; discussion ONSE174.
10. Kermer C, Rasse M, Lagogiannis G, Undt G, Wagner A, Millesi W. Color stereolithography for planning complex maxillofacial tumor surgery. J Craniomaxillofac Surg 1998 Dec;26(6):360-362.
11. Undt G, Wild K, Reuther G, Ewers R. MRI-based stereolithographic models of the temporomandibular joint: technical innovation. J Craniomaxillofac Surg 2000 Oct;28(5):258-263.
12. Islam S, Walton GM, Dean F, Hoffman GR. Multidisciplinary management of a complicated orbital injury inflicted by a horse. Ophthal Plast Reconstr Surg 2007 Nov-Dec;23(6):486-488.
13. Kermer C, Lindner A, Friede I, Wagner A, Millesi W. Preoperative stereolithographic model planning for primary reconstruction in craniomaxillofacial trauma surgery. J Craniomaxillofac Surg 1998 Jun;26(3):136-139.
14. Powers DB, Edgin WA, Tabatchnick L. Stereolithography: a historical review and indications for use in the management of trauma. J Craniomaxillofac Trauma 1998 Fall;4(3):16-23.
15. Klug C, Schicho K, Ploder O, Yerit K, Watzinger F, Ewers R, Baumann A, Wagner A. Point-to-point computer-assisted navigation for precise transfer of planned zygoma osteotomies from the stereolithographic model into reality. J Oral Maxillofac Surg 2006 Mar;64(3):550-559.
16. Sailer HF, Haers PE, Zollikofer CP, Warnke T, Carls FR, Stucki P. The value of stereolithographic models for preoperative diagnosis of craniofacial deformities and planning of surgical corrections. Int J Oral Maxillofac Surg 1998 Oct;27(5):327-333.
17. Zhou L, He L, Shang H, Liu G, Zhao J, Liu Y. Correction of hemifacial microsomia with the help of mirror imaging and a rapid prototyping technique: case report. Br J Oral Maxillofac Surg 2009 Sep;47:486-488.
18. Pelo S, Tassiello S, Boniello R, Gasparini G, Longobardi G. A new method for assessment of craniofacial malformations. J Craniofac Surg 2006 Nov;17(6):1035-1039.
19. Sinn DP, Cillo JE Jr, Miles BA. Stereo-lithography for craniofacial surgery. J Craniofac Surg 2006 Sep;17(5): 869-875.
20. Uemura T, Hayashi T, Furukawa Y, Mitsukawa N, Yoshikawa A, Jinnai T. Surgical program for

craniosynostosis using three-dimensional solid model, combined with autologous blood transfusion in a Japanese craniofacial unit. J Craniofac Surg 2001 Sep;12(5):479-484.
21. Sakurai A, Hirabayashi S, Sugawara Y, Harii K. Skeletal analysis of craniofacial deformities in brachycephaly: comparison with craniofacial deformities in plagiocephaly. Scand J Plast Reconstr Surg Hand Surg 2001 Jun;35(2):165-175.
22. Lin CC, Lo LJ, Lee MY, Wong HF, Chen YR. Craniofacial surgical simulation: application of three-dimensional medical imaging and rapid prototyping models. Chang Gung Med J 2001 Apr;24(4):229-238.
23. Eppley BL, Sadove AM. Computer-generated patient models for reconstruction of cranial and facial deformities. J Craniofac Surg 1998 Nov;9(6):548-556.
24. Kreiborg S, Dahl E. Cranial base and face in mandibulofacial dysostosis. Am J Med Genet 1993 Oct;47(5):753-760.
25. Wong TY, Fang JJ, Chung CH, Huang JS, Lee JW. Comparison of 2 methods of making surgical models for correction of facial asymmetry. J Oral Maxillofac Surg 2005 Feb;63(2):200-208.
26. Zhou LB, Shang HT, He LS, Bo B, Liu GC, Liu YP, Zhao JL. Accurate reconstruction of discontinuous mandible using a reverse engineering/computer-aided design/rapid prototyping technique: a preliminary clinical study. J Oral Maxillofac Surg 2010 Sep;68(9):2115-2121.
27. Nakajima T, Yoshimura Y, Nakanishi Y, Koga S, Katada K. Integrated life-sized solid model of bone and soft tissue: application for cleft lip and palate infants. Plast Reconstr Surg 1995 Oct;96(5):1020-1025.
28. Al-Ani SA, Locke MB, Rees M, de Chalain TM. Our experiences managing a rare cranio-orbital cleft. J Craniofac Surg 2008 May;19(3):819-822.
29. Chen XY, Chen SL, Zhang X, Li JP, Deng W. Accuracy of intraoral vertical ramus osteotomy with a stereolithographic template. Ann Plast Surg 2011 Jan;66(1):88-91.
30. Bai S, Bo B, Bi Y, Wang B, Zhao J, Liu Y, Feng Z, Shang H, Zhao Y. CAD/CAM surface templates as an alternative to the intermediate wafer in orthognathic surgery. Oral Surg Oral Med Oral Pathol Oral Radiol Endod 2010 Nov;110(5):e1-7.
31. Hibi H, Sawaki Y, Ueda M. Three-dimensional model simulation in orthognathic surgery. Int J Adult Orthodon Orthognath Surg 1997;12(3):226-232.
32. Hoffmann J, Schwaderer E, Dammann F. The use of hybrid stereolithographic models for the planning of complex craniofacial procedures. Biomed Tech (Berl) 2002;47(Suppl 1Pt1):278-281.
33. Gateno J, Xia JJ, Teichgraeber JF, Christensen AM, Lemoine JJ, Liebschner MA, Gliddon MJ, Briggs ME. Clinical feasibility of computer-aided surgical simulation (CASS) in the treatment of complex cranio-maxillofacial deformities. J Oral Maxillofac Surg 2007 Apr;65(4):728-734.
34. Whitman DH, Connaughton B. Model surgery prediction for mandibular midline distraction osteogenesis. Int J Oral Maxillofac Surg 1999 Dec;28(6):421-423.
35. Robiony M, Salvo I, Costa F, Zerman N, Bazzocchi M, Toso F, Bandera C, Filippi S, Felice M, Politi M. Virtual reality surgical planning for maxillofacial distraction osteogenesis: the role of reverse engineering rapid prototyping and cooperative work. J Oral Maxillofac Surg 2007 Jun;65(6):1198-1208.
36. Poukens J, Haex J, Riediger D. The use of rapid prototyping in the preoperative planning of distraction osteogenesis of the cranio-maxillofacial skeleton. Comput Aided Surg 2003;8(3):146-154.
37. Minami K, Mori Y, Tae-Geon K, Shimizu H, Ohtani M, Yura Y. Maxillary distraction osteogenesis in cleft lip and palate patients with skeletal anchorage. Cleft Palate Craniofac J 2007 Mar;44(2):137-141.
38. Varol A, Basa S. The role of computer-aided 3D surgery and stereolithographic modelling for vector orientation in premaxillary and trans-sinusoidal maxillary distraction osteogenesis. Int J Med Robot 2009 Jun;5(2):198-206.

39. Yamaji KE, Gateno J, Xia JJ, Teichgraeber JF. New internal Le Fort I distractor for the treatment of midface hypoplasia. J Craniofac Surg 2004 Jan;15(1):124-127.
40. Robiony M. Distraction osteogenesis: a method to improve facial balance in asymmetric patients. J Craniofac Surg 2010 Mar;21(2):508-512.
41. Feiyun P, Wei L, Jun C, Xin X, Zhuojin S, Fengguo Y. Simultaneous correction of bilateral temporomandibular joint ankylosis with mandibular micrognathia using internal distraction osteogenesis and 3-dimensional craniomaxillofacial models. J Oral Maxillofac Surg 2010 Mar;68(3):571-577.
42. Lethaus B, Kessler P, Boeckman R, Poort LJ, Tolba R. Reconstruction of a maxillary defect with a fibula graft and titanium mesh using CAD/CAM techniques. Head Face Med 2010 Jul;19(6):16.
43. Eisele DW, Richtsmeier WJ, Graybeal JC, Koch WM, Zinreich SJ. Three-dimensional models for head and neck tumor treatment planning. Laryngoscope 1994 Apr;104(4):433-439.
44. He Y, Zhu HG, Zhang ZY, He J, Sader R. Three-dimensional model simulation and reconstruction of composite total maxillectomy defects with fibula osteomyocutaneous flap flow-through from radial forearm flap. Oral Surg Oral Med Oral Pathol Oral Radiol Endod 2009 Dec;108(6):e6-12.
45. Al-Sukhun J, Törnwall J, Lindqvist C, Kontio R, Penttila H. One-stage zygomaticomandibular approach for improved access to the hemimaxilla and the middle base of the skull. J Craniofac Surg 2008 Mar;19(2):528-533.
46. Ekstrand K, Hirsch JM. Malignant tumors of the maxilla: virtual planning and real-time rehabilitation with custom-made R-zygoma fixtures and carbon-graphite fiber-reinforced polymer prosthesis. Clin Implant Dent Relat Res 2008 Mar;10(1):23-29.
47. Matsuo A, Chiba H, Takahashi H, Toyoda J, Abukawa H. Clinical application of a custom-made bioresorbable raw particulate hydroxyapatite/poly-L-lactide mesh tray for mandibular reconstruction. Odontology 2010 Feb;98(1):85-88.
48. Cohen A, Laviv A, Berman P, Nashef R, Abu-Tair J. Mandibular reconstruction using stereolithographic 3-dimensional printing modeling technology. Oral Surg Oral Med Oral Pathol Oral Radiol Endod 2009 Nov;108(5):661-666.
49. Kernan BT, Wimsatt JA 3rd. Use of a stereolithography model for accurate, preoperative adaptation of a reconstruction plate. J Oral Maxillofac Surg 2000 Mar;58(3):349-351.
50. Dziegielewski PT, Zhu J, King B, Grosvenor A, Dobrovolsky W, Singh P, Ansari K, Al-Qahtani KH, Harris JR, Seikaly H. Three-dimensional biomodeling in complex mandibular reconstruction and surgical simulation: prospective trial. J Otolaryngol Head Neck Surg 2011 Feb;40 Suppl 1:S70-81.
51. Yamashita Y, Yamaguchi Y, Tsuji M, Shigematsu M, Goto M. Mandibular reconstruction using autologous iliac bone and titanium mesh reinforced by laser welding for implant placement. Int J Oral Maxillofac Implants 2008 Nov-Dec;23(6):1143-1146.
52. Liu XJ, Gui L, Mao C, Peng X, Yu GY. Applying computer techniques in maxillofacial reconstruction using a fibula flap: a messenger and an evaluation method. J Craniofac Surg 2009 Mar;20(2):372-377.
53. Hutchison IL, Dawood A, Tanner S. Immediate implant supported bridgework simultaneous with jaw reconstruction for a patient with mandibular osteosarcoma. Br Dent J 2009 Feb 14;206(3):143-146.
54. Ortakoglu K, Akcam T, Sencimen M, Karakoc O, Ozyigit HA, Bengi O. Osteochondroma of the mandible causing severe facial asymmetry: a case report. Oral Surg Oral Med Oral Pathol Oral Radiol Endod 2007 May;103(5):e21-e28.
55. Asaumi J, Kawai N, Honda Y, Shigehara H, Wakasa T, Kishi K. Comparison of three-dimensional computed tomography with rapid prototype models in the management of coronoid hyperplasia. Dentomaxillofac Radiol 2001 Nov;30(6):330-335.

56. Mainenti P, Oliveira GS, Valério JB, Daroda LS, Daroda RF, Brandão G, Rosa LE. Ameloblastic fibro-odontosarcoma: a case report. Int J Oral Maxillofac Surg 2009 Mar;38(3):289-292.
57. Zhang S, Liu X, Xu Y, Yang C, Undt G, Chen M, Haddad MS, Yun B. Application of rapid prototyping for temporomandibular joint reconstruction. J Oral Maxillofac Surg 2011 Feb;69(2):432-438.
58. Worrall SF, Christensen RW. Alloplastic reconstruction of the temporomandibular joint in treatment of craniofacial developmental or congenital anomalies: a surgical case report. Surg Technol Int 2006;15:291-301.
59. Zizelmann C, Bucher P, Rohner D, Gellrich NC, Kokemueller H, Hammer B. Virtual restoration of anatomic jaw relationship to obtain a precise 3D models for total joint prosthesis construction for treatment of TMJ ankylosis with open bite. Int J Oral Maxillofac Surg 2010 Oct;39(10):1012-1015.
60. Müller A, Krishnan KG, Uhl E, Mast G. The application of rapid prototyping techniques in cranial reconstruction and preoperative planning in neurosurgery. J Craniofac Surg 2003 Nov;14(6):899-914.
61. Dattilo DJ, Bursick D. Management of traumatic cranial vault deformities using three-dimensional computer-generated models. J Trauma 1994 May;36(5):691-694.
62. Arnaud E, Marchac D, Renier D. Aplasia of the vertex without scalp defect. J Craniofac Surg 1997 Mar;8(2):146-150.
63. Lo LJ, Chen YR, Tseng CS, Lee MY. Computer-aided reconstruction of traumatic fronto-orbital osseous defects: aesthetic considerations. Chang Gung Med J 2004 Apr;27(4):283-291.
64. Bill JS, Reuther JF, Dittmann W, Kübler N, Meier JL, Pistner H, Wittenberg G. Stereolithography in oral and maxillofacial operation planning. Int J Oral Maxillofac Surg 1995 Feb;24(1 Pt 2):98-103.
65. Cao D, Yu Z, Chai G, Liu J, Mu X. Application of EH compound artificial bone material combined with computerized three-dimensional reconstruction in craniomaxillofacial surgery. J Craniofac Surg 2010 Mar;21(2):440-443.
66. Kübler N, Michel C, Zöller J, Bill J, Mühling J, Reuther J. Repair of human skull defects using osteoinductive bone alloimplants. J Craniomaxillofac Surg 1995 Dec;23(6):337-346.
67. Wu CT, Lee ST, Chen JF, Lin KL, Yen SH. Computer-aided design for three-dimensional titanium mesh used for repairing skull base bone defect in pediatric neurofibromatosis type 1. A novel approach combining biomodeling and neuronavigation. Pediatr Neurosurg 2008;44(2):133-139.
68. Cillo JE Jr, Theodotou N, Samuels M, Krajekian J. The tent pole splint: a bone-supported stereolithographic surgical splint for the soft tissue matrix expansion graft procedure. J Oral Maxillofac Surg 2010 Jun;68(6):1365-1370.
69. Vrielinck L, Politis C, Schepers S, Pauwels M, Naert I. Image-based planning and clinical validation of zygoma and pterygoid implant placement in patients with severe bone atrophy using customized drill guides. Preliminary results from a prospective clinical follow-up study. Int J Oral Maxillofac Surg 2003 Feb;32(1):7-14.
70. Frühwald J, Schicho KA, Figl M, Benesch T, Watzinger F, Kainberger F. Accuracy of craniofacial measurements: computed tomography and three-dimensional computed tomography compared with stereolithographic models. J Craniofac Surg 2008 Jan;19(1):22-26.
71. Chang PS, Parker TH, Patrick CW Jr, Miller MJ. The accuracy of stereolithography in planning craniofacial bone replacement. J Craniofac Surg 2003 Mar;14(2):164-170.
72. Schicho K, Figl M, Seemann R, Ewers R, Lambrecht JT, Wagner A, Watzinger F, Baumann A, Kainberger F, Fruehwald J, Klug C. Accuracy of treatment planning based on stereolithography in computer assisted surgery. Med Phys 2006 Sep;33(9):3408-3459.
73. Kragskov J, Sindet-Pedersen S, Gyldensted C, Jensen KL. A comparison of three-dimensional computed tomography scans and stereolithographic models for evaluation of

craniofacial anomalies. J Oral Maxillofac Surg 1996 Apr;54(4):402-411, discussion 411-412.
74. D'Urso PS, Barker TM, Earwaker WJ, Bruce LJ, Atkinson RL, Lanigan MW, Arvier JF, Effeney DJ. Stereolithographic biomodelling in cranio-maxillofacial surgery: a prospective trial. J Craniomaxillofac Surg 1999 Feb;27(1):30-37.
75. Cheung LK, Wong MC, Wong LL. Refinement of facial reconstructive surgery by stereo model planning. Ann R Australas Coll Dent Surg 2002 Oct;16:129-132.
76. Arvier JF, Barker TM, Yau YY, D'Urso PS, Atkinson RL, McDermant GR. Maxillofacial biomodelling. Br J Oral Maxillofac Surg 1994 Oct;32(5):276-283.
77. Korves B, Klimek L, Klein HM, Mösges R. Image and model-based surgical planning in otolaryngology. J Otolaryngol 1995 Oct;24(5):265-270.
78. Murray DJ, Edwards G, Mainprize JG, Antonyshyn O. Optimizing craniofacial osteotomies: applications of haptic and rapid prototyping technology. J Oral Maxillofac Surg 2008 Aug;66(8):1766-1772.
79. Lo LJ, Chen YR. Three-dimensional computed tomography imaging in craniofacial surgery: morphological study and clinical applications. Chang Gung Med J 2003 Jan;26(1):1-11.
80. Yau YY, Arvier JF, Barker TM. Technical note: maxillofacial biomodelling--preliminary result. Br J Radiol 1995 May;68(809):519-523.
81. Sannomiya EK, Silva JV, Brito AA, Saez DM, Angelieri F, Dalben Gda S. Surgical planning for resection of an ameloblastoma and reconstruction of the mandible using a selective laser sintering 3D biomodel. Oral Surg Oral Med Oral Pathol Oral Radiol Endod 2008 Jul;106(1):e36-40.
82. Leiggener C, Messo E, Thor A, Zeilhofer HF, Hirsch JM. A selective laser sintering guide for transferring a virtual plan to real time surgery in composite mandibular reconstruction with free fibula osseous flaps. Int J Oral Maxillofac Surg 2009 Feb;38(2):187-192.
83. Aung SC, Tan BK, Foo CL, Lee ST. Selective laser sintering: application of a rapid prototyping method in craniomaxillofacial reconstructive surgery. Ann Acad Med Singapore 1999 Sep;28(5):739-743.
84. Li WZ, Zhang MC, Li SP, Zhang LT, Huang Y. Application of computer-aided three-dimensional skull model with rapid prototyping technique in repair of zygomatico-orbito-maxillary complex fracture. Int J Med Robot 2009 Jun;5(2):158-163.
85. Williams JV, Revington PJ. Novel use of an aerospace selective laser sintering machine for rapid prototyping of an orbital blowout fracture. Int J Oral Maxillofac Surg 2010 Feb;39(2):182-184.
86. Rotaru H, Baciut M, Stan H, Bran S, Chezan H, Iosif A, Tomescu M, Kim SG, Rotaru A, Baciut G. Silicone rubber mould cast polyethylmethacrylate-hydroxyapatite plate used for repairing a large skull defect. J Craniomaxillofac Surg 2006 Jun;34(4):242-246.
87. da Rosa EL, Oleskovicz CF, Aragão BN. Rapid prototyping in maxillofacial surgery and traumatology: case report. Braz Dent J 2004;15(3):243-247.
88. Sannomiya EK, Reis SA, Asaumi J, Silva JV, Barbara AS, Kishi K. Clinical and radiographic presentation and preparation of the prototyping models for pre-surgical planning in Apert's syndrome. Dentomaxillofac Radiol 2006 Mar;35(2):119-124.
89. Silva DN, Gerhardt de Oliveira M, Meurer E, Meurer MI, Lopes da Silva JV, Santa-Barbara A. Dimensional error in selective laser sintering and 3D-printing of models for craniomaxillary anatomy reconstruction. J Craniomaxillofac Surg 2008 Dec;36(8):443-449.
90. Ibrahim D, Broilo TL, Heitz C, de Oliveira MG, de Oliveira HW, Nobre SM, Dos Santos Filho JH, Silva DN. Dimensional error of selective laser sintering, three-dimensional printing and PolyJet models in the reproduction of mandibular anatomy. J Craniomaxillofac Surg 2009 Apr;37(3):167-173.
91. Sohmura T, Kusumoto N, Otani T, Yamada S, Wakabayashi K, Yatani H. CAD/CAM fabrication and clinical application of surgical template and bone model in oral implant surgery. Clin Oral Implants Res 2009 Jan;20(1):87-93.

92. Kozakiewicz M, Elgalal M, Loba P, Komunski P, Arkuszewski P, Broniarczyk-Loba A, Stefanczyk L. Clinical application of 3D pre-bent titanium implants for orbital floor fractures. J Craniomaxillofac Surg 2009 Jun;37(4):229-234.
93. Kozakiewicz M, Elgalal M, Piotr L, Broniarczyk-Loba A, Stefanczyk L. Treatment with individual orbital wall implants in humans - 1-Year ophthalmologic evaluation. J Craniomaxillofac Surg 2011 Jan;39(1):30-36.
94. Mavili ME, Canter HI, Saglam-Aydinatay B, Kamaci S, Kocadereli I. Use of three-dimensional medical modeling methods for precise planning of orthognathic surgery. J Craniofac Surg 2007 Jul;18(4):740-747.
95. Olszewski R, Tranduy K, Reychler H. Innovative procedure for computer-assisted genioplasty: three-dimensional cephalometry, rapid prototyping model and surgical splint. Int J Oral Maxillofac Surg 2010 Jul;39(7):721-724.
96. Klammert U, Böhm H, Schweitzer T, Würzler K, Gbureck U, Reuther J, Kübler A. Multi-directional Le Fort III midfacial distraction using an individual prefabricated device. J Craniomaxillofac Surg 2009 Jun;37(4):210-215.
97. Schön R, Metzger MC, Zizelmann C, Weyer N, Schmelzeisen R. Individually preformed titanium mesh implants for a true-to-original repair of orbital fractures. Int J Oral Maxillofac Surg 2006 Nov;35(11):990-995.
98. Olszewski R, Reychler H, Cosnard G, Denis JM, Vynckier S, Zech F. Accuracy of three-dimensional (3D) craniofacial cephalometric landmarks on a low-dose 3D computed tomograph. Dentomaxillofac Radiol 2008 Jul;37(5):261-267.
99. Scolozzi P, Momjian A, Heuberger J, Andersen E, Broome M, Terzic A, Jaques B. Accuracy and predictability in use of AO three-dimensionally preformed titanium mesh plates for posttraumatic orbital reconstruction: a pilot study. J Craniofac Surg 2009 Jul;20(4):1108-1113.
100. Ewers R, Schicho K. Augmented reality telenavigation in cranio-maxillofacial oral surgery. Stud Health Technol Inform 2009;150:24-25.
101. Bell RB, Markiewicz MR. Computer-assisted planning, stereolithographic modeling, and intraoperative navigation for complex orbital reconstruction: a descriptive study in a preliminary cohort. J Oral Maxillofac Surg 2009 Dec;67(12):2559-2570.
102. Ayoub AF, Stirrups DR, Moos KF. Assessment of chin surgery by a coordinate free method. Int J Oral Maxillofac Surg 1994 Feb;23(1):6-10.
103. Olszewski R, Zech F, Cosnard G, Nicolas V, Macq B, Reychler H. Three-dimensional computed tomography cephalometric craniofacial analysis: Experimental validation in vitro. Int J Oral Maxillofac Surg 2007 Sep;36(9):828-833.
104. Husami T, Leffler K, Churnik R, Lehman JA Jr. Sterilization of the bone pencil. Plast Reconstruct Surg 1988 Dec;82(6):1100.
105. Xia J, Ip HH, Samman N, Wang D, Kot CS, Yeung RW, Tideman H. Computer-assisted three-dimensional surgical planning and simulation: 3D virtual osteotomy. Int J Oral Maxillofac Surg 2000 Feb;29(1):11-17.
106. Ewers R, Schicho K, Wagner A, Undt G, Seemann R, Figl M, Truppe M. Seven years of clinical experience with teleconsultation in craniomaxillofacial surgery. J Oral Maxillofac Surg 2005 Oct;63(10):1447-1454.
107. Santler G, Karcher H, Ruda C. Indications and limitations of three-dimensional models in cranio-maxillofacial surgery. J Craniomaxillofac Surg 1998 Feb;26(1):11-16.
108. Olszewski R, Reychler H. Three-dimensional surgical guide for frontal-nasal-ethmoid-vomer disjunction in Le Fort III osteotomy. J Craniofac Surg 2011 Sep;22(5):1791-1792.
109. Epker BN, Wolford LM. Dentofacial deformities. Surgical-orthodontic correction. Mosby Ed, St Louis, Toronto, London, 1980.
110. Nout E, Cesteleyn LL, van der Wal KG, van Adrichem LN, Mathijssen IM, Wolvius EB. Advancement of the midface, from conventional Le Fort III osteotomy to Le Fort III distraction: review of the literature. Int J Oral Maxillofac Surg 2008 Sep;37(9):781-789.
111. Gosain AK, Santoro TD, Havlik RJ, Cohen SR, Holmes RE. Midface distraction following

Le Fort III and monobloc osteotomies: problems and solutions. Plast Reconstr Surg 2002 May;109(6):1797-1808.
112. Matsumoto K, Nakanishi H, Seike T, Koizumi Y, Hirabayashi S. Intracranial hemorrhage resulting from skull base fracture as a complication of Le Fort III osteotomy. J Craniofac Surg 2003 Jul;14(4):545-548.
113. Jeelani NU, Khan MA, Fitzgerald O'Connor EJ, Dunaway D, Hayward R. Frontofacial monobloc distraction using the StealthStation intraoperative navigation system: the ability to see where you are cutting. J Craniofac Surg 2009 May;20(3):892-894.
114. Song SJ, Choi J, Park YD, Lee JJ, Hong SY, Sun K. A three-dimensional bioprinting system for use with a hydrogel-based biomaterial and printing parameter characterization. Artif Organs 2010 Nov;34(11):1044-1048.
115. Jakab K, Norotte C, Marga F, Murphy K, Vunjak-Novakovic G, Forgacs G. Tissue engineering by self-assembly and bio-printing of living cells. Biofabrication 2010 Jun;2(2):022001.
116. Mironov V, Boland T, Trusk T, Forgacs G, Markwald RR. Organ printing: computer-aided jet-based 3D tissue engineering. Trends Biotechnol 2003 Apr;21(4):157-161.
117. Mironov V, Kasyanov V, Markwald RR. Organ printing: from bioprinter to organ biofabrication line. Curr Opin Biotechnol 2011 Oct;22(5):667-67.